Increased particle and energy transport induced by LH waves in the tokamak scrape-off layer plasma

V. Pericoli Ridolfini

Associaz. EURATOM-ENEA sulla Fusione, CR Frascati, CP 65, 00044 Frascati, Roma, Italy

Introduction. This work deals with the physics of the interaction of the lower hybrid (LH) waves with the tokamak edge plasma in order to help foreseeing correctly both the behaviour of the waves in the main plasma and the consequences of the induced variations for the first wall materials. The paper focuses on the modifications of the scrape-off layer (SOL) turbulence and on what this implies for the average SOL conditions, namely density, n_e, and temperature, T_e. It describes the experimental observations and interprets them on the basis of simple physics arguments with the aim to provide useful inputs for future modelling work.

Experimental equipment and findings. Two series of 8 Langmuir electrodes, fixed at both sides of each of the two LH antennas [1] (matrix 4×2) collect the FTU SOL local data. 4 of them are biased in c.c. to measure the ion saturation current, $I_{sat,i} \propto n_e \cdot c_s = n_e \cdot [m_i/(T_i+T_e)]^{1/2}$ and its fluctuations, $\delta I_{sat,i}$, at 500 kHz rate [2] (c_s=ion sound velocity, $m_i(m_e)$=ion (electron) mass). Even if the contributions of n_e and T_e cannot be discriminated, $\delta I_{sat,i}$ will be often confused with δn_e, as justified by local measurements of δn_e, δT_e, δV_p (plasma potential) [3] in FTU. The other 12 electrodes sample the average T_e and n_e every 2 ms, from a standard single electrode I-V (current-voltage) characteristics. The values at LCMS (last closed magnetic surface) are so derived: $T_{e,LCMS}$ from the Thomson scattering, $n_{e,LCMS}$ from the inversion of the multi-chord CO_2 scanning interferometer data, [4]. The values in between LCMS and the electrodes are calculated from an exponential decay law that is usually observed in FTU [2].

A large step forward in the knowledge of the SOL fluctuations has been the ability to estimate its typical perpendicular wave vector, ξ_t, from the correlation between two electrodes with the same poloidal angle θ on either side of the LH grill. Because of the magnetic shear and of the slight mismatch between the actual LCMS shape and the antenna profile, the corresponding flux tubes are $h_\perp \approx 6$ mm apart in the perpendicular direction. The "parallel" distance is totally neglected since a perfect coherence is assumed along the filed lines, i.e. $\xi_\parallel = 0$ and coherence length, $\lambda_{coh,\parallel} = \infty$. More details can be found in Ref. [5]. An example of the correlation function Γ during the LHCD phase and OH phase is shown in Fig. 1. The dashed vertical lines mark the average delay time τ_Γ as the centre of mass of the cross-correlation function, calculated for $-500 < \tau < 500$ μs and $\Gamma > 0.65 \cdot \Gamma_{max}$. The cross-correlation is always at the noise level for any other couple, with or w/o the LH power. From the r.m.s. fluctuation frequency value, ω_t, one has $\xi_t = \omega_t \tau_\Gamma / h_\perp$. The results are shown in Fig. 2 from a scan of the line-averaged density, $\bar{n}_e$, as the plot of $\xi_t \rho_{i,L}$ ($\rho_{i,L}$=ion Larmor radius=$(2m_iT_i)^{1/2}/(qB_T)$ q=electron charge) versus $n_{e,LCMS}$ in LH and OH phases. OH data show no clear trend with $n_{e,LCMS}$, if we consider that the errors are the same as in LH (the possible decrease could derive from the lower $\rho_{i,L}$ due to lower T_e), while the LH values increase almost linearly. They are largely above OH mostly due to higher ξ_t, since the increase of T_e produces only a factor ≈1.6.

The following data have been obtained through a scan of the main plasma parameters in the ranges: $0.65 \leq \bar{n}_e \leq 1.55 \times 10^{20}$ m^{-3}, $0.35 \leq I_p \leq 0.6$ MA, $5.2 \leq B_{T0} \leq 7.2$ T.

The main features of the fluctuations are more closely linked to the local conditions of the SOL, than of the bulk ones. Here are presented only the most convincing ones. In addition to T_e and n_e, important is also the magnetic topology, which was independently varied by operating the (usually) secondary poloidal limiter as the primary one, instead of the toroidal limiter. This lengthens the connection lengths, L_{con}, by about a factor 3.

The next Fig. 4 plots the LH and OH relative fluctuation levels, rms($\delta I_{sat,i}/I_{sat,i}$), versus the product of the e^- collision frequency, ν_{ee}, by the particle dwell time in the flux tube, τ_{dwell}, $\nu_{ee} \times \tau_{dwell}$=total number of collisions suffered by the particles during their lifetime. Both quantities are calculated from the average T_e and n_e values inferred from the Langmuir electrodes working inside this tube. Considering this 'normalized' collisionality rather than ν_{ee} alone is mandatory if one wants to maintain together the data from normal and lengthened L_{con} values. Again, the separation between LH and OH cases is clear. For LH a strong drop of from an asymptotic OH value of ≈23% down to ≈10% is observed at high collisionality.

The LH induced effects are mainly bounded inside the flux tube defined by the excited grill, inside which the distance has no effect. Perpendicularly the variation is large, as the following figures will show. The data are extracted from the lowest, the middle and the highest density discharge of a series where only $\bar{n}_e$ was varied, and are presented as the ratio of LH to OH values versus θ, poloidal distance from the LH grill. In Fig. 3, the increase of p_e (e^- pressure) with LH is mainly due to T_e. It is close to a factor 4 at θ=0 for #32323, the highest density discharge, with a T_e increases by ≈3.3 times. A clear variation all over the θ range that lasts the whole LH pulse, is seen only for #32323, even though this is not immediately inferred from the plot. For the lowest density, instead, the effect drops already on the second electrode much more than for the other two cases. In Fig. 5, $\delta I_{sat,i}/I_{sat,i}$ is plotted versus θ. Again the effects are larger for the highest $\bar{n}_e$: the ratio drops by about a factor 2 on the first two electrodes, while is ≈1 on the farthest ones. The quite low effect at the lowest density already at θ=0 makes it more difficult to recognize the spreading along θ that occurs as $\bar{n}_e$ increases.

The next Fig. 6 summarizes the variations that the LH waves induce in the energy transport in the SOL, by plotting the e-folding of the power flow $p_e \cdot c_s$, $\lambda_{q\|}=1/(1/\lambda_n+1/\lambda_T^{3/2})$ versus θ. Its magnitude can increase up to 1.4-1.5 times due to LH, which is of great relevance for possible mitigation of the power loads on the divertor targets.

Discussion – The figures here presented show how the SOL turbulence is strongly affected by the LH waves. The effects it has in turn on the LH properties are dealt with elsewhere [6]. The average fluctuation wave vector increase (Fig. 2) is interpreted as due to he need to maintain unchanged the total momentum in the multiple collisions with LH waves. Indeed, its magnitude follows that of the LH wave vector: $k_{0,LH}=k_{\|,LH} \cdot \omega_{pe}/\omega_0$ ($\omega_{pe}/2\pi$=electron plasma frequency=$89.8\sqrt{n_e}$[10^{20}m^{-3}] GHz, $k_{\|,LH}$=launched parallel wave vector ≈Δφ/b for a Δφ phasing between adjacent waveguides separated by the length b). The growth is faster than

$\sqrt{n}_{eLCMS}$, maybe due to the more numerous collisions occurring with slower waves ($v_\perp = \omega_0/k_{0,LH}$). Higher sloshing energy of the particles, $W_{slsh}=1/2\varepsilon_0 E_{||}(\omega_{pe}/\omega_0)^2$ is also available to draw more power into the fluctuations, as suggested by the fact that the increment of the absolute level is $\Delta(\text{rms}(\delta I_{sat,i})) \approx 2\times10^{-3}$, 1.2×10^{-2}, 0.1 A, starting from OH levels $\approx 1.6\times10^{-2}$, 1.6×10^{-2}, 0.15 A, for the lowest, the middle and the highest point, respectively.

An advanced non-linear modelling, which is in project, could explain the different saturation levels and the stabilizing effect of the collisionality (Fig. 4). This latter is consistent with the usual increase of the SOL fluctuations when approaching the walls and density drops [7].

The modifications of the SOL turbulence induced by the LH waves affect both the particle and energy transport, as inferred from the variations of the decay lengths. This comparison is however not trivial since the λ values derive from the balance between the perpendicular and parallel transport, which in turn are interdependent through the velocity c_s. Consistently with the statement that Δp_e in front of the grill is mainly due to T_e and less to n_e, the λ_T increase is definitely larger than λ_n, which, on the contrary, λ_n can even decrease. This however can be understood in the light of he expression for λ_n in a turbulence-dominated transport [3]: $\lambda_n = 2L_{con}\xi_t V_p(<\delta n_e/n_e)^2+<\delta V_p/V_p>^2)^{1/2}\Gamma_{n,V}(0)/(c_s B_T)$, $\Gamma_{n,V}(0)$ is the cross-correlation between δn_e and δV_p for null delay. Taking as an example the high density case, #32323, the variation of a factor ≈6 on ξ_t, due to LH, is partially balanced by the reduction in the fluctuation level, which gives a factor ≈0.3 in the approximation $\delta V_p/V_p \approx \delta n_e/n_e$ [3], and in $\Gamma_{n,V}$, which gives a factor ≈0.5-0.6 or even smaller when the auto-correlation times drops substantially [3], as in our case where τ_{self} drops from about 30 to 3 μs. The product of the these three factors is ≈ 1.1, but clearly slight changes can even shorten λ_n. Substantially, then, the particle diffusion coefficient $D_\perp$ remains unchanged. On the other side, the λ_T increase under the LH action is driven by the ratio $\Gamma_{T,V}(0)/\Gamma_{n,V}(0)$ [5, 3] and then it is accounted for by the fact that $\Gamma_{T,V}(0)$ remains almost unchanged. The derived estimate for the thermal diffusion is $\chi_{e\perp,LH}/\chi_{e\perp,OH} \approx 5$.

Conclusions. The FTU SOL turbulence is largely affected by the injection of LH power in all its main features, level, frequency, power spectrum, and perpendicular wave vector. The local LCMS density and the normalized collisionality propose as the governing parameters. This latter has a stabilizing effect on the turbulent process, while $n_{e,LCMS}$ determines the wave vector of the LH waves, which in turn affect the SOL turbulence through multiple scattering. The consequences are large for the thermal diffusion - λ_T changes by a factor ≈2.5, whereas they are not large for the particle diffusion - λ_n is almost unchanged. The resulting decay length of the power flow rises by a factor ≈1.5, which is a relevant figure in view of the problem of mitigating the power loads on divertor targets in future reactors. A quite important step forward towards controlling the particle and heat fluxes on the divertor targets would be understanding the reason why these modifications spread outside the LH flux tube. Possibly both a wave lower accessibility and a higher SOL optical thickness would retain a larger fraction of the injected power ‘trapped’ in the edge, and available for modifying the SOL turbulence. Should this second hypothesis be dominant, it would be a sound promise for

enhancing the transport in the SOL, hence for mitigating the power loads, because the optical thickness increases noticeably as frequency decreases. This would mean lower overall costs.

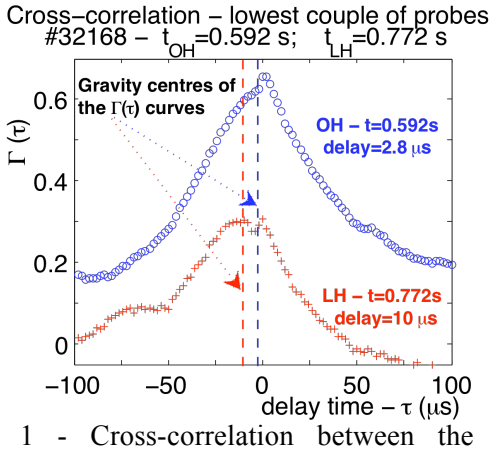

Fig. 1 - Cross-correlation between the two Langmuir electrodes on the LH antenna, θ≈-26°

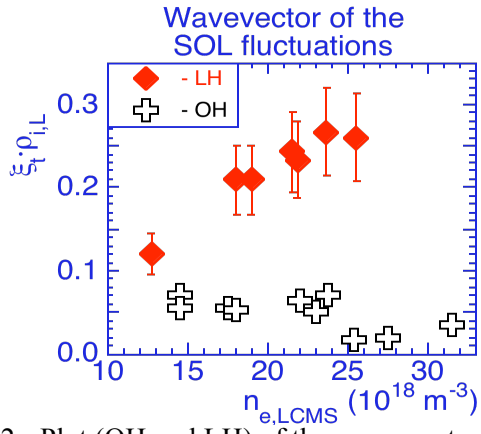

Fig. 2 - Plot (OH and LH) of the wave-vector vs. density at LCMS

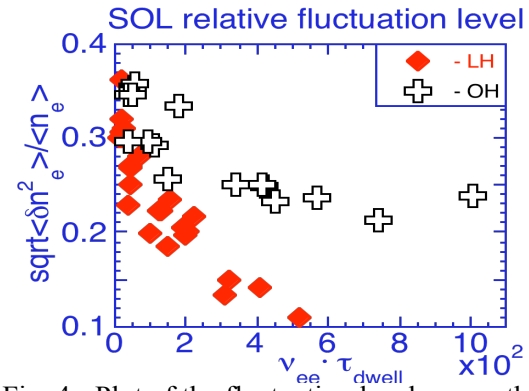

Fig. 4 - Plot of the fluctuation level versus the normalised collisionality

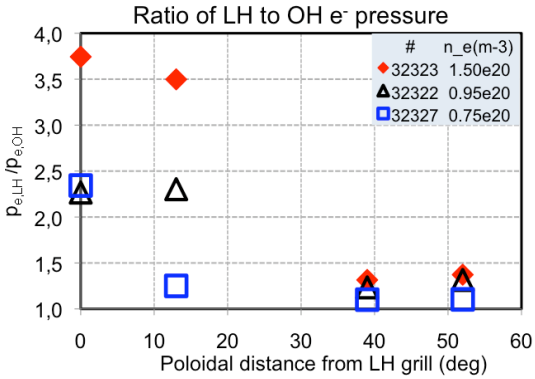

Fig. 3 - LH to OH e^- pressure ratio in front of the LH antenna vs. the angular distance from the excited grill

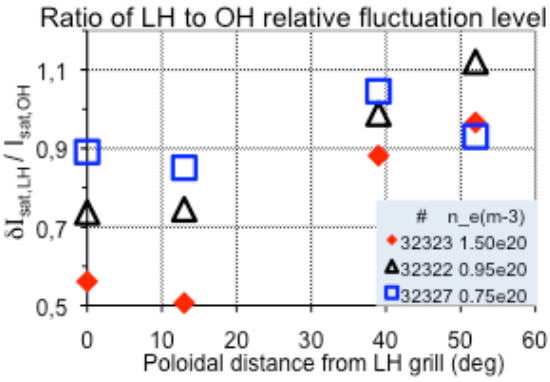

Fig. 5 - Relative fluctuation level ratio, LH to OH, in front of the LH antenna as a function of the angular distance from the excited grill

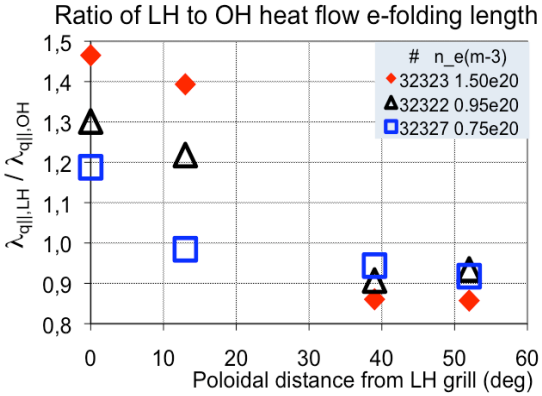

Fig. 6 - e-folding length of the parallel power flow, ratio of LH to OH values, as a function of the poloidal distance from the excited grill

REFERENCES

[1] M. Aquilini et al., Fus Sci & Tech, **V. 45**, p. 459, ch. 11, May 2004
[2] V. Pericoli Ridolfini et al., J. Nucl. Mat. **V. 220-222**, p. 218-222 (1995)
[3] V. Pericoli Ridolfini et al., Nucl. Fus., **V. 38**, p. 1745-1755 (1998)
[4] O. Tudisco et al., Fus Sci & Tech, **V. 45**, p. 402, ch. 8, May 2004
[5] V. Pericoli Ridolfini et al., work in preparation
[6] V. Pericoli Ridolfini et al., paper P5.176, this conference
[7] V. Pericoli Ridolfini et al., Nucl. Fus., **V. 34**, p. 469-481, (1994)